



Natural convective boundary-layer flow of a nanofluid past a vertical plate

A.V. Kuznetsov^{a,*}, D.A. Nield^b

^a Department of Mechanical and Aerospace Engineering, North Carolina State University, Campus Box 7910, Raleigh, NC 27695-7910, USA

^b Department of Engineering Science, University of Auckland, Private Bag 92019, Auckland 1142, New Zealand

ARTICLE INFO

Article history:

Received 22 April 2009

Received in revised form

15 July 2009

Accepted 15 July 2009

Available online 14 August 2009

Keywords:

Nanofluid

Brownian motion

Thermophoresis

Natural convection

Boundary layer

Vertical plate

ABSTRACT

The natural convective boundary-layer flow of a nanofluid past a vertical plate is studied analytically. The model used for the nanofluid incorporates the effects of Brownian motion and thermophoresis. A similarity solution is presented. This solution depends on a Lewis number Le , a buoyancy-ratio number Nr , a Brownian motion number Nb , and a thermophoresis number Nt . For various values of Pr and Le , the variation of the reduced Nusselt number with Nr , Nb and Nt is expressed by correlation formulas. It was found that the reduced Nusselt number is a decreasing function of each of Nr , Nb and Nt .

© 2009 Elsevier Masson SAS. All rights reserved.

1. Introduction

The term “nanofluid” refers to a liquid containing a suspension of submicronic solid particles (nanoparticles). The term was coined by Choi [1]. The characteristic feature of nanofluids is thermal conductivity enhancement, a phenomenon observed by Masuda et al. [2]. This phenomenon suggests the possibility of using nanofluids in advanced nuclear systems (Buongiorno and Hu [3]).

A comprehensive survey of convective transport in nanofluids was made by Buongiorno [4], who says that a satisfactory explanation for the abnormal increase of the thermal conductivity and viscosity is yet to be found. He focused on the further heat transfer enhancement observed in convective situations. Buongiorno notes that several authors have suggested that convective heat transfer enhancement could be due to the dispersion of the suspended nanoparticles but he argues that this effect is too small to explain the observed enhancement. Buongiorno also concludes that turbulence is not affected by the presence of the nanoparticles so this cannot explain the observed enhancement. Particle rotation has also been proposed as a cause of heat transfer enhancement, but Buongiorno calculates that this effect is too small to explain the

effect. With dispersion, turbulence and particle rotation ruled out as significant agencies for heat transfer enhancement, Buongiorno proposed a new model based on the mechanics of the nanoparticle/base-fluid relative velocity.

Buongiorno [4] noted that the nanoparticle absolute velocity can be viewed as the sum of the base fluid velocity and a relative velocity (that he calls the slip velocity). He considered in turn seven slip mechanisms: inertia, Brownian diffusion, thermophoresis, diffusiophoresis, Magnus effect, fluid drainage, and gravity settling. After examining each of these in turn, he concluded that in the absence of turbulent effects it is the Brownian diffusion and the thermophoresis that will be important. Buongiorno proceeded to write down conservation equations based on these two effects.

The problem of natural convection in a regular fluid past a vertical plate is a classical problem first studied theoretically by E. Pohlhausen in a contribution to an experimental study by Schmidt and Beckmann [5]. Unfortunately the boundary-layer scaling used by early researchers and text book authors did not properly incorporate the dependence on the Prandtl number. Exceptions are provided by the papers by Kuiken [6,7]. The situation was clarified by Bejan [8]. An extension to the case of heat and mass transfer was made by Khair and Bejan [9].

In this paper we extend the study of the Pohlhausen–Kuiken–Bejan problem to the case of a nanofluid using the model of Buongiorno [4]. A similarity solution is obtained.

* Corresponding author. Tel.: +1 919 515 5292; fax: +1 919 515 7968.

E-mail addresses: avkuznet@eos.ncsu.edu (A.V. Kuznetsov), d.nield@auckland.ac.nz (D.A. Nield).

Nomenclature		\mathbf{v}	velocity, (u, v)
D_B	Brownian diffusion coefficient	(x, y)	Cartesian coordinates (x -axis is aligned vertically upwards, plate is at $y = 0$)
D_T	thermophoretic diffusion coefficient		
f	rescaled nanoparticle volume fraction, defined by Eq. (20)		
\mathbf{g}	gravitational acceleration vector		
k	thermal conductivity		
Le	Lewis number, defined by Eq. (28)		
Nr	buoyancy-ratio parameter, defined by Eq. (25)		
Nb	Brownian motion parameter, defined by Eq. (26)		
Nt	thermophoresis parameter, defined by Eq. (27)		
Nu	Nusselt number, defined by Eq. (31)		
Nur	reduced Nusselt number, $Nu/Ra_x^{1/4}$		
Pr	Prandtl number, defined by Eq. (24)		
p	pressure		
q''	wall heat flux		
Ra_x	local Rayleigh number, defined by Eq. (18)		
s	dimensionless stream function, defined by Eq. (20)		
T	temperature		
T_w	temperature at the vertical plate		
T_∞	ambient temperature attained as y tends to infinity		
			<i>Greek symbols</i>
		α	thermal diffusivity
		β	volumetric expansion coefficient of the fluid
		η	similarity variable, defined by Eq. (19)
		θ	dimensionless temperature, defined by Eq. (20)
		μ	dynamic viscosity of the fluid
		ν	kinematic viscosity, $\mu/\rho_{f\infty}$
		ρ_f	fluid density
		ρ_p	nanoparticle mass density
		$(\rho c)_f$	heat capacity of the fluid
		$(\rho c)_p$	effective heat capacity of the nanoparticle material
		τ	parameter defined by Eq. (13), $(\rho c)_p/(\rho c)_f$
		ϕ	nanoparticle volume fraction
		ϕ_w	nanoparticle volume fraction at the vertical plate
		ϕ_∞	ambient nanoparticle volume fraction attained as y tends to infinity
		ψ	stream function, defined by Eq. (14)

2. Analysis

We consider a two-dimensional problem. We select a coordinate frame in which the x -axis is aligned vertically upwards. We consider a vertical plate at $y = 0$. At this boundary the temperature T and the nanoparticle fraction ϕ take constant values T_w and ϕ_w , respectively. The ambient values, attained as y tends to infinity, of T and ϕ are denoted by T_∞ and ϕ_∞ , respectively.

The Oberbeck–Boussinesq approximation is employed. The following four field equations embody the conservation of total mass, momentum, thermal energy, and nanoparticles, respectively. The field variables are the velocity \mathbf{v} , the temperature T and the nanoparticle volume fraction ϕ .

$$\nabla \cdot \mathbf{v} = 0, \tag{1}$$

$$\rho_f \left(\frac{\partial \mathbf{v}}{\partial t} + \mathbf{v} \cdot \nabla \mathbf{v} \right) = -\nabla p + \mu \nabla^2 \mathbf{v} + \left[\phi \rho_p + (1 - \phi) \left\{ \rho_f (1 - \beta(T - T_\infty)) \right\} \right] \mathbf{g}, \tag{2}$$

$$(\rho c)_f \left(\frac{\partial T}{\partial t} + \mathbf{v} \cdot \nabla T \right) = k \nabla^2 T + (\rho c)_p [D_B \nabla \phi \cdot \nabla T + (D_T/T_\infty) \nabla T \cdot \nabla T], \tag{3}$$

$$\frac{\partial \phi}{\partial t} + \mathbf{v} \cdot \nabla \phi = D_B \nabla^2 \phi + (D_T/T_\infty) \nabla^2 T. \tag{4}$$

We write $\mathbf{v} = (u, v)$.

Here ρ_f is the density of the base fluid and μ, k and β are the density, viscosity, thermal conductivity and volumetric volume expansion coefficient of the nanofluid, while ρ_p is the density of the particles. The gravitational acceleration is denoted by \mathbf{g} . The coefficients that appear in Eqs. (3) and (4) are the Brownian diffusion coefficient D_B and the thermophoretic diffusion coefficient D_T . Details of the derivation of Eqs. (3) and (4) are given in the papers by Buongiorno [4] and Nield and Kuznetsov [10,11].

The boundary conditions are taken to be

$$u = 0, \quad v = 0, \quad T = T_w, \quad \phi = \phi_w \quad \text{at } y = 0, \tag{5}$$

$$u = v = 0, \quad T \rightarrow T_\infty, \quad \phi \rightarrow \phi_\infty \quad \text{as } y \rightarrow \infty. \tag{6}$$

We consider a steady state flow.

In keeping with the Oberbeck–Boussinesq approximation and an assumption that the nanoparticle concentration is dilute, and with a suitable choice for the reference pressure, we can linearize the momentum equation and write equation (2) as

$$\rho_f \left(\frac{\partial \mathbf{v}}{\partial t} + \mathbf{v} \cdot \nabla \mathbf{v} \right) = -\nabla p + \mu \nabla^2 \mathbf{v} + \left[(\rho_p - \rho_{f\infty}) (\phi - \phi_\infty) + (1 - \phi_\infty) \rho_{f\infty} \beta (T - T_\infty) \right] \mathbf{g}. \tag{7}$$

We now make the standard boundary-layer approximation, based on a scale analysis, and write the governing equations

$$\frac{\partial u}{\partial x} + \frac{\partial v}{\partial y} = 0, \tag{8}$$

$$\frac{\partial p}{\partial x} = \mu \frac{\partial^2 u}{\partial y^2} - \rho_f \left(u \frac{\partial u}{\partial x} + v \frac{\partial u}{\partial y} \right) + \left[(1 - \phi_\infty) \rho_{f\infty} \beta g (T - T_\infty) - (\rho_p - \rho_{f\infty}) g (\phi - \phi_\infty) \right] \tag{9}$$

$$\frac{\partial p}{\partial y} = 0, \tag{10}$$

$$u \frac{\partial T}{\partial x} + v \frac{\partial T}{\partial y} = \alpha \nabla^2 T + \tau \left[D_B \frac{\partial \phi}{\partial y} \frac{\partial T}{\partial y} + \left(\frac{D_T}{T_\infty} \right) \left(\frac{\partial T}{\partial y} \right)^2 \right], \tag{11}$$

$$u \frac{\partial \phi}{\partial x} + v \frac{\partial \phi}{\partial y} = D_B \frac{\partial^2 \phi}{\partial y^2} + \left(\frac{D_T}{T_\infty} \right) \frac{\partial^2 T}{\partial y^2}. \tag{12}$$

where

$$\alpha = \frac{k}{(\rho C)_f}, \quad \tau = \frac{(\rho C)_p}{(\rho C)_f} \tag{13}$$

One can eliminate p from Eqs. (9) and (10) by cross-differentiation. At the same time one can introduce a stream function ψ defined by

$$u = \frac{\partial \psi}{\partial y}, \quad v = -\frac{\partial \psi}{\partial x}, \tag{14}$$

so that Eq. (8) is satisfied identically.

We are then left with the following three equations.

$$\frac{\partial \psi}{\partial y} \frac{\partial^2 \psi}{\partial x \partial y} - \frac{\partial \psi}{\partial x} \frac{\partial^2 \psi}{\partial y^2} - \nu \frac{\partial^3 \psi}{\partial y^3} = (1 - \phi_\infty) \rho_{f\infty} \beta g (T - T_\infty) - (\rho_p - \rho_{f\infty}) g \phi \tag{15}$$

$$\frac{\partial \psi}{\partial y} \frac{\partial T}{\partial x} - \frac{\partial \psi}{\partial x} \frac{\partial T}{\partial y} = \alpha \nabla^2 T + \tau \left[D_B \frac{\partial \phi}{\partial y} \frac{\partial T}{\partial y} + \left(\frac{D_T}{T_\infty} \right) \left(\frac{\partial T}{\partial y} \right)^2 \right], \tag{16}$$

$$\frac{\partial \psi}{\partial y} \frac{\partial \phi}{\partial x} - \frac{\partial \psi}{\partial x} \frac{\partial \phi}{\partial y} = D_B \frac{\partial^2 \phi}{\partial y^2} + \left(\frac{D_T}{T_\infty} \right) \frac{\partial^2 T}{\partial y^2}. \tag{17}$$

In deriving Eq. (15) an integration with respect to y has been performed, and use has been made of the boundary conditions at infinity. Here $\nu = \mu/\rho_{f\infty}$.

We now introduce the local Rayleigh number Ra_x defined by

$$Ra_x = \frac{(1 - \phi_\infty) \beta g (T_w - T_\infty) x^3}{\nu \alpha}, \tag{18}$$

and the similarity variable

$$\eta = \frac{y}{x} Ra_x^{1/4}. \tag{19}$$

This choice is made on the basis of scale analysis. Since most nanofluids examined to date have large values for the Lewis number Le , we are interested mainly in the case $Le > 1$. Also we are interested in the case where it is heat transfer (rather than mass

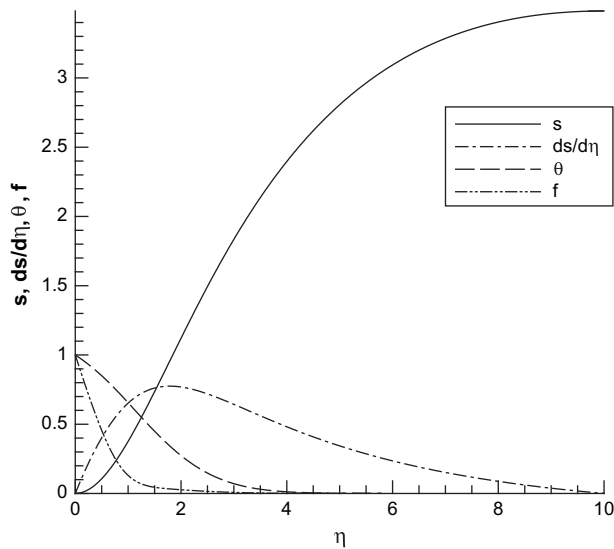


Fig. 1. Plots of dimensionless similarity functions $s(\eta)$, $ds(\eta)/d\eta$, $\theta(\eta)$, $f(\eta)$ for the case $Pr = 10$, $Le = 10$, $Nr = 0.5$, $Nb = 0.5$, $Nt = 0.5$. These represent the distributions of stream function, longitudinal velocity, temperature, and nanoparticle volume fraction, respectively.

Table 1

Comparison test results. Values of the reduced Nusslet number $Nur = Nu/Ra_x^{1/4}$ in the limiting case of a regular fluid. The present results are with $\eta_{max} = 10$, $Le = 10$, $Nr = Nb = Nt = 10^{-5}$.

Pr	1	10	100	1000
Nur (Bejan [8])	0.401	0.465	0.490	0.499
Nur (present)	0.401	0.463	0.481	0.484

transfer) that is driving the flow. In the present context this means that we are assuming that the buoyancy-ratio parameter Nr defined by Eq. (25) below is small compared with unity and that the Lewis number Le defined by Eq. (28) is larger than unity.

We also introduce the dimensionless variables s , θ , and f defined by

$$s(\eta) = \frac{\psi}{\alpha Ra_x^{1/4}}, \quad \theta(\eta) = \frac{T - T_\infty}{T_w - T_\infty}, \quad f(\eta) = \frac{\phi - \phi_\infty}{\phi_w - \phi_\infty}. \tag{20}$$

Then, on substitution in Eqs. (15–17), we obtain the ordinary differential equations

$$s''' + \frac{1}{4Pr} (3ss'' - 2s'^2) + \theta - Nr f = 0, \tag{21}$$

$$\theta'' + \frac{3}{4}s\theta' + Nb f' \theta' + Nt \theta'^2 = 0, \tag{22}$$

$$f'' + \frac{3}{4}Les f' + \frac{Nt}{Nb} \theta'' = 0, \tag{23}$$

where the five parameters are defined by

$$Pr = \frac{\nu}{\alpha}, \tag{24}$$

$$Nr = \frac{(\rho_p - \rho_{f\infty})(\phi_w - \phi_\infty)}{\rho_{f\infty} \beta (T_w - T_\infty)(1 - \phi_\infty)}, \tag{25}$$

$$Nb = \frac{(\rho C)_p D_B (\phi_w - \phi_\infty)}{(\rho C)_f \alpha}, \tag{26}$$

$$Nt = \frac{(\rho C)_p D_T (T_w - T_\infty)}{(\rho C)_f \alpha T_\infty}, \tag{27}$$

$$Le = \frac{\alpha}{D_B}. \tag{28}$$

Here Nr , Nb , Nt , Le denote a buoyancy ratio, a Brownian motion parameter, a thermophoresis parameter, and a Lewis number, respectively.

Equations (21–23) are solved subject to the following boundary conditions:

Table 2a

Case $Le = 10$. Linear regression coefficients and error bound for the reduced Nusslet number. Here C_r , C_b , C_t , are the coefficients in the linear regression estimate $Nu_{est}/Ra_x^{1/4} = Nur_{PKB} + C_r Nr + C_b Nb + C_t Nt$, and ϵ is the maximum relative error defined by $\epsilon = |(Nu_{est} - Nu)/Nu|$, applicable for Nr , Nb , Nt each in $[0, 0.5]$. Variation with Prandtl number is displayed.

Pr	Nur_{PKB}	C_r	C_b	C_t	ϵ
1	0.401	-0.047	-0.224	-0.137	0.083
2	0.465	-0.055	-0.256	-0.160	0.084
5	0.490	-0.064	-0.271	-0.172	0.098
10	0.499	-0.071	-0.279	-0.180	0.111

Table 2b

Case Pr = 10. Linear regression coefficients and error bound for the reduced Nusselt number, as for Table 2a. Variation with Lewis number is displayed.

Le	Nur _{PKB}	C _r	C _b	C _t	ε
5	0.465	-0.076	-0.224	-0.162	0.085
10	0.465	-0.055	-0.256	-0.160	0.084

At $\eta = 0$: $s = 0, s' = 0, \theta = 1, f = 1.$ (29)

As $\eta \rightarrow \infty$: $s' = 0, \theta = 0, f = 0.$ (30)

When Nr, Nb and Nt are all zero, Eqs. (21) and (22) involve just two dependent variables, namely s and θ , and the boundary-value problem for these two variables reduces to the classical Pohlhausen–Kuiken–Bejan problem. (The boundary-value problem for f then becomes ill-posed and is of no physical significance).

A quantity of practical interest is the Nusselt number Nu defined by

$$Nu = \frac{q''x}{k(T_w - T_\infty)}, \tag{31}$$

where q'' is the wall heat flux. In the present context $Nu/Ra_x^{1/4}$ (something that we shall refer to as the reduced Nusselt number and denote by Nur) is represented by $-\theta'(0)$. (Likewise the dimensionless mass flux is represented by a Sherwood number Sh proportional to $-f'(0)$, but this of lesser interest here).

3. Results and discussion

The Pohlhausen–Kuiken–Bejan (PKB) problem for a regular fluid involves just one independent dimensionless parameter, namely the Prandtl number, Pr. The present extension involves four more independent dimensionless parameters: Le, Nr, Nb, and Nt. Hence we need to be very selective in our choice of parameter values. It is also imperative that the computational time for each set of input parameter values should be short. One source of error is inevitable, because the physical domain is unbounded whereas the computational domain has to be finite. One has to apply the far field boundary conditions at a finite value of the similarity variable η here denoted by η_{max} . We ran our bulk calculations with the value $\eta_{max} = 10$. We compared the resulting calculated values for the special case of a regular fluid with those reported in Table 4.2 in Bejan [8], with the results shown in Table 1. The error becomes worse as Pr increases, and our computed value is about 3% too small when Pr = 1000. Since our main objective is to explore the influence of the parameters Le, Nr, Nb and Nt, we regard a systematic error of this magnitude as acceptable for our present purpose.

We will present the results of our investigation of the effect of the parameters Nr, Nb and Nt on Nur, for various values of Pr and Le.

Plots of the dependent similarity variables for a typical case, chosen as that for Pr = 10, Le = 10, Nr = 0.5, Nb = 0.5, Nt = 0.5, are shown in Fig. 1. The boundary-layer profiles for the temperature function $\theta(\eta)$ and the stream function $s(\eta)$ have essentially the same form as in the case of a regular fluid. As one would expect, the

thermal boundary-layer thickness is less than the momentum boundary-layer thickness when Pr > 1. The thickness of the boundary-layer for the mass fraction function $f(\eta)$ is smaller than the thermal boundary-layer thickness when Le > 1. We have checked that these profiles change little as the parameters Nr, Nb and Nt are varied.

For the case Pr = 10, Le = 10, the value of $Nu/Ra_x^{1/4}$ (something that we will refer to as the reduced Nusselt number and denote by Nur) was calculated for 125 sets of values of Nr, Nb, Nt in the range [0.1, 0.2, 0.3, 0.4, 0.5] and a linear regression was performed on the results. This yielded the correlation

$$Nur_{est} = 0.465 - 0.055Nr - 0.256Nb - 0.160Nt, \tag{32}$$

valid for Nr, Nb, Nt each taking values in the range [0, 0.5], with a maximum error of about 8%. Clearly an increase in any of the buoyancy-ratio number Nr, the Brownian motion parameter Nb, or the thermophoresis parameter Nt leads to a decrease in the value of the reduced Nusselt number (corresponding to an increase in the thermal boundary-layer thickness). The maximum error occurs at the extreme end of the range considered, namely when (Nr, Nb, Nt) = (0.5, 0.5, 0.5), and the correlation formula overestimates the reduction from the standard fluid value 0.465.

This exercise was repeated for other values of Pr and Le, with the results shown in Tables 2a and 2b. (We found numerical difficulty with small (close to unity) and very large values of Le so the variation with Le is circumscribed.) These results show that the coefficient of Nt varies little as Le varies. This result is to be expected since, from the form of Eq. (23), one can anticipate that when Le is large the variable f' will decay rapidly as η increases, and then since the term in Nt in Eq. (22) does not involve f one can anticipate that the contribution from Nt will not depend markedly on the value of Le. On the other hand, the magnitude of the coefficient of Nr decreases markedly as Le increase while the magnitude of the coefficient of Nt changes in the other direction. Finally from comparison with Table 1 we observe that the accuracy of the linear regression estimate increases as Le increases but decreases as Pr increases.

We believe that for most practical purposes the simple linear regression formula in Eq. (32) should be adequate. If one wants a more accurate formula then one can perform a quadratic regression. For the case Pr = 10, Le = 10, for example, we obtained instead of Eq. (32) the formula

$$\begin{aligned} Nur_{est} = & 0.465 - 0.052Nr - 0.312Nb - 0.201Nt - 0.001Nr^2 \\ & + 0.035Nb^2 + 0.047Nt^2 + 0.128NbNt - 0.002NtNr \\ & + 0.071NrNb, \end{aligned} \tag{33}$$

which gives a maximum error of just 0.9% over the same range. The relatively large interactions between Nr and Nb (displayed by the coefficient of the last term in Eq. (33)), and between Nb and Nt (displayed by the coefficient of the third to last term in Eq. (33)) are of interest. Values of the coefficients for some other cases are presented in Tables 3a and 3b.

Table 3a

Case Le = 10. Quadratic regression coefficients and error bound for the reduced Nusselt number. Here C_{r1}, C_{r2}, C_{b1}, C_{b2}, C_{t1}, C_{t2}, C_{br}, C_{tr} and C_{rb} are the coefficients in the quadratic regression estimate $Nu_{est}/Ra_x^{1/2} = Nur_{PKB} + C_{r1}Nr + C_{b1}Nb + C_{t1}Nt + C_{r2}Nr^2 + C_{b2}Nb^2 + C_{t2}Nt^2 + C_{br}NbNt + C_{tr}NtNr + C_{rb}NrNb$, and ε is the maximum relative error defined by $\epsilon = |(Nu_{est} - Nu)/Nu|$, applicable for Nr, Nb, Nt each in [0, 0.5]. Variation with Prandtl number is displayed.

Pr	Nur _{PKB}	C _{r1}	C _{b1}	C _{t1}	C _{r2}	C _{b2}	C _{t2}	C _{br}	C _{tr}	C _{rb}	ε
1	0.401	-0.041	-0.273	-0.171	-0.002	0.031	0.038	0.111	-0.005	0.060	0.009
10	0.465	-0.052	-0.312	-0.201	0.001	0.035	0.047	0.128	-0.002	0.071	0.009
100	0.490	-0.071	-0.337	-0.224	0.016	0.047	0.062	0.145	-0.009	0.087	0.013
1000	0.499	-0.086	-0.354	-0.241	0.028	0.059	0.075	0.157	0.020	0.099	0.019

Table 3bCase $Pr = 10$. Linear regression coefficients and error bound for the reduced Nusselt number, as for Table 2a. Variation with Lewis number is displayed.

Le	Nu_{PKB}	C_{r1}	C_{b1}	C_{t1}	C_{r2}	C_{b2}	C_{t2}	C_{bt}	C_{tr}	C_{rb}	ε
5	0.465	-0.079	-0.262	-0.204	-0.009	0.034	0.046	0.149	-0.023	0.129	0.024
10	0.465	-0.052	-0.312	-0.201	0.001	0.035	0.047	0.128	-0.002	0.071	0.009

4. Conclusions

We have examined the influence of nanoparticles on natural convection boundary-layer flow past a vertical plate, using a model in which Brownian motion and thermophoresis are accounted for. In this pioneering study we have assumed the simplest possible boundary conditions, namely those in which both the temperature and the nanoparticle fraction are constant along the wall. This permits a simple similarity solution which depends on five dimensionless parameters, namely a Prandtl number Pr , a Lewis number Le , a buoyancy-ratio parameter Nr , a Brownian motion parameter Nb , and a thermophoresis parameter Nt . We have explored the way in which the wall heat flux, represented by a Nusselt number Nu and then scaled in terms of $Ra_x^{1/4}$ to produce a reduced Nusselt number, depends on these five parameters. Since we are dealing with the case of convection driven mainly by heat transfer we expect that the boundary condition on the nanoparticle fraction is of lesser importance. Our prime result is that the reduced Nusselt number is a decreasing function of each of nanofluid numbers Nr , Nb and Nt .

References

- [1] S. Choi, Enhancing thermal conductivity of fluids with nanoparticle in: D.A. Siginer, H.P. Wang (Eds.), *Developments and Applications of Non-Newtonian Flows*, ASME MD vol. 231 and FED vol. 66, 1995, pp. 99–105.
- [2] H. Masuda, A. Ebata, K. Teramae, N. Hishinuma, Alteration of thermal conductivity and viscosity of liquid by dispersing ultra-fine particles, *Netsu Bussei* 7 (1993) 227–233.
- [3] J. Buongiorno, W. Hu, Nanofluid coolants for advanced nuclear power plants, Paper no. 5705, Proceedings of ICAPP '05, Seoul, May 15–19, 2005.
- [4] J. Buongiorno, Convective transport in nanofluids, *ASME J. Heat Transf.* 128 (2006) 240–250.
- [5] E. Schmidt, W. Beckmann, Das temperatur- und geschwindigkeitsfeld von einer wärme abgebenden senkrechten platte bei natürlicher konvektion, II. die versuche und ihre ergebnisse, *Forch. Ingenieurwes* 1 (1930) 391–406.
- [6] H.K. Kuiken, An asymptotic solution for large Prandtl number free convection, *J. Eng. Math.* 2 (1968) 355–371.
- [7] H.K. Kuiken, Free convection at low Prandtl numbers, *J. Fluid Mech.* 39 (1969) 785–798.
- [8] A. Bejan, *Convection Heat Transfer*, Wiley, New York, NY, 1984.
- [9] K.R. Khair, A. Bejan, Mass transfer to natural convection boundary-layer flow driven by heat transfer, *ASME J. Heat Transf.* 107 (1985) 979–981.
- [10] D.A. Nield, A.V. Kuznetsov, The onset of convection in a nanofluid layer, *ASME J. Heat Transf.*, submitted for publication.
- [11] D.A. Nield, A.V. Kuznetsov, Thermal instability in a porous medium layer saturated by a nanofluid, *Int. J. Heat Mass Transf.*, in press.